

Accelerated Light-Induced Degradation (ALID) for Monitoring of Defects in PV Silicon Wafers and Solar Cells

MARSHALL WILSON,¹ PIOTR EDELMAN,^{1,2} ALEXANDRE SAVTCHOUK,¹
JOHN D'AMICO,¹ ANDREW FINDLAY,¹ and JACEK LAGOWSKI¹

1.—Semilab SDI LLC., 3650 Spectrum Boulevard, Suite 130, Tampa, FL 33612, USA. 2.—e-mail: piotr.edelman@semilabsdi.com

In crystalline silicon, above-bandgap illumination can transform defects into strong recombination centers, degrading minority-carrier lifetime and solar cell efficiency. This light-induced degradation (LID) is due primarily to boron–oxygen and iron–boron defects, and can be reversed using thermal treatments that are distinctly different for each type of defect. Combining illumination and thermal treatment, we have designed an accelerated light-induced degradation (ALID) cycle that, within minutes, transforms defects into the distinct states needed to isolate individual contributions from boron–oxygen dimers (BO_{2i}) and interstitial iron (Fe_i). In this cycle, the concentrations of BO_{2i} and Fe_i are determined using surface photovoltage (SPV) diffusion length measurement. The ALID cycle uses reversible defect reactions and gives very good repeatability of wafer-scale mapping of BO_{2i} and Fe_i in photovoltaic (PV) wafers and final solar cells.

Key words: Silicon, photovoltage, contamination, PV, defects, boron–oxygen dimer, full wafer mapping, light degradation, solar cells

INTRODUCTION

Noncontact measurement of alternating potential (AC) surface photovoltage (SPV) is commonly used for determining the minority-carrier diffusion length L . Such a measurement is done with a transparent pick-up electrode capacitively coupled to the wafer. In the constant-photon-flux SPV method employed in this study, two SPV signals are measured simultaneously using two intensity-modulated monochromatic light beams slightly shifted in modulation frequency. The two beams have different wavelengths, giving different light penetration depths, z . The L value is extracted by fitting the SPV signal ratio to a theoretical expression. A detailed description is available in Refs. 1 and 2 and references therein.

A very low injection level makes the AC SPV minority-carrier diffusion length the most sensitive measure of recombination centers in silicon. In the

present work, AC SPV has been applied for quantitative measurement of recombination defects in crystalline Si photovoltaic wafers and solar cells, with an emphasis on light-induced degradation (LID) of lifetime, open-circuit voltage, and efficiency. The boron–oxygen and iron–boron defects shown in Fig. 1 are the two key centers that contribute to LID in crystalline Si.^{3–5}

The goal of this study is to develop an accelerated light-induced degradation (ALID) procedure for fast defect transformation to preselected states corresponding to different recombination activities. Three of these states are listed in Table I. For simplicity, we use the terms “not active” and “active” to refer to defect states corresponding to reduced and enhanced recombination activity, respectively.

For both defects the light-induced transformation to a high recombination state is attributed to photoinjected electrons. In the case of an iron–boron pair it is the liberation of an interstitial Fe_i donor (Fig. 1). The pair dissociation reaction involves a recombination-enhanced process in which the electron transition from the conduction band to the

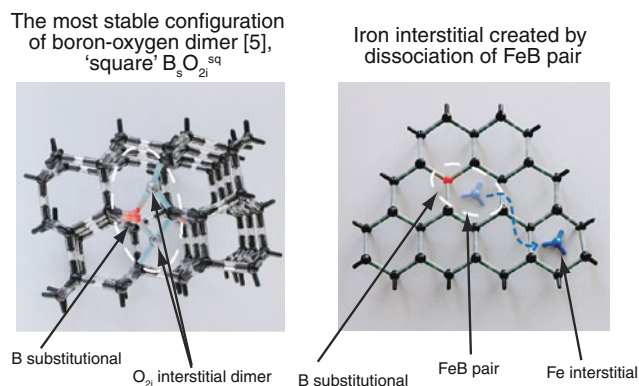


Fig. 1. Two defects in the Si lattice that change their recombination efficiency upon above-bandgap illumination.

Table I. Selected defect states for ALID measurements

State 1	BO_{2i} not active	Fe not active
State 2	BO_{2i} active	Fe not active
State 3	BO_{2i} active	Fe active

$E_v + 0.1$ eV level of the pair provides energy, helping to split the electrostatically bonded donor-acceptor $Fe_1^+-B^-$ pair.³ In the boron-oxygen defect, the BO_{2i} complex shown in Fig. 1 acts as a highly effective recombination center. It is believed that the diffusivity of the oxygen dimer, O_{2i} , is enhanced by the photoinjected electrons, leading to the room-temperature association reaction $B + O_{2i} \rightarrow BO_{2i}$.

O_{2i} diffusivity increases with temperature, as does the rate of BO_{2i} formation. With increasing temperature, however, a reverse reaction starts to dominate, transferring BO_{2i} to an inactive state. The reverse reaction for Fe_i (i.e., the pairing of Fe and B) occurs at a much lower temperature than the deactivation of BO_{2i} , enabling selective engineering of weak recombination states of these defects.

Selected defect transformations to states in Table I can be achieved in minutes, using elevated temperature and two types of wafer illumination. Short high-intensity flash light pulses preferentially activate Fe_i at room temperature. Lower intensity but longer halogen illumination at elevated temperature preferentially activates BO_{2i} . Brief annealings at 200°C and 90°C are used to deactivate BO_{2i} and Fe_i , respectively.

An automated ALID apparatus uses robotic handling to transfer wafers between processing platforms, loading/unloading platforms, and an AC SPV measuring stage for diffusion length mapping. Measurements reported in this paper were obtained with an automated commercial C.FORS series ALID and AC SPV tool developed by Semilab SDI.

RESULTS AND DISCUSSION

Diffusion length maps measured on an as-cut multicrystalline p -Si wafer prior to solar cell processing at three different defect states created by ALID are shown in Fig. 2. The largest diffusion length, with an average value of 103.6 μm is observed for state 1, in which BO_{2i} and Fe are not activated. ALID activation of BO_{2i} defects into state 2 decreases the average L to 75.4 μm . A further decrease in diffusion length, to 63.7 μm , is observed for state 3, when both defects are active.

The concentration of activated defects is proportional to the corresponding change of $1/L^2$. The proportionality constant depends on the minority-carrier diffusivity and defect capture cross-section in the active and inactive states. The diffusion length difference between state 2 and state 3 is caused by the activation of iron, and the iron concentration in atoms/cm³ is therefore determined using the well-known expression⁶ used in commercial SPV Fe measuring tools:

$$[Fe_i] = \frac{1.05e16}{\left(\frac{1}{L_3^2} - \frac{1}{L_2^2}\right)}, \quad (1)$$

where L_2 and L_3 are the diffusion length values in μm measured in states 2 and 3, respectively. The capture cross-sections for active and inactive BO_{2i} states are not known with sufficient certainty to determine the absolute concentration of boron-oxygen dimers. We therefore adopt an "iron equivalent" concentration that assumes capture coefficients the same as those for iron. This procedure is commonly used in the SPV measurement of recombination centers other than iron.¹ This "iron equivalent" concentration of boron-oxygen dimers per cm³ is obtained by:

$$[BO_{2i}] = \frac{1.05e16}{\left(\frac{1}{L_2^2} - \frac{1}{L_1^2}\right)}, \quad (2)$$

where L_1 and L_2 are the diffusion length values in μm measured in states 1 and 2, respectively.

The maps of $[BO_{2i}]$ and $[Fe_i]$ shown in Fig. 3 were obtained from the diffusion length maps in Fig. 2. They demonstrate the different spatial distributions of these two defects. In the photovoltaic cell manufacturing sequence, iron can be removed from the p -type base region by the phosphorous diffusion step used to form the n^+ emitter layer. However, phosphorous gettering may not be effective if the initial Fe concentration is very high (i.e., above 10^{13} atoms/cm³).

To control cell manufacturing, these measurements should be done on both as-cut wafers and processed wafers, including final solar cells. In this respect, ALID and SPV diffusion length measurements are applicable to Si photovoltaic wafers at various stages of cell manufacturing. Results of

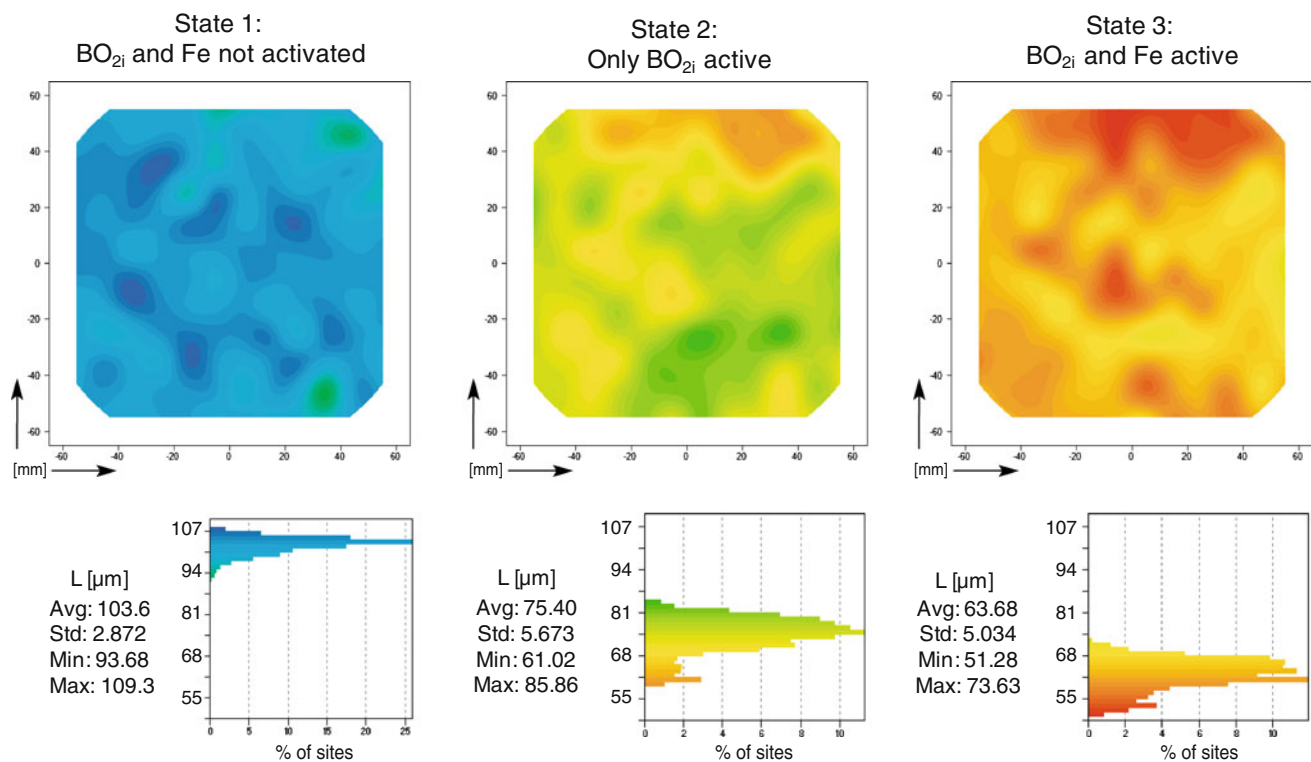


Fig. 2. AC SPV diffusion length maps of multicrystalline wafers in different states of defect recombination activity.

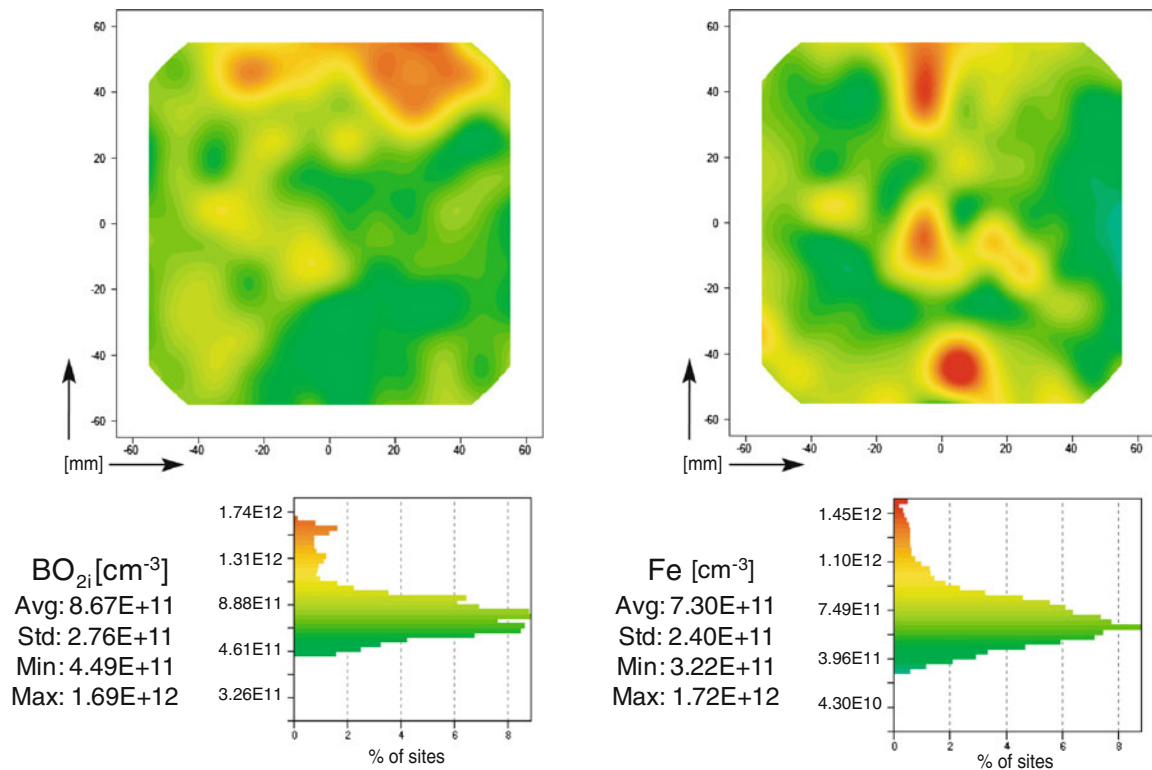


Fig. 3. Maps of BO_{2i} and Fe concentrations in a multicrystalline Si wafer, obtained from the data in Fig. 2.

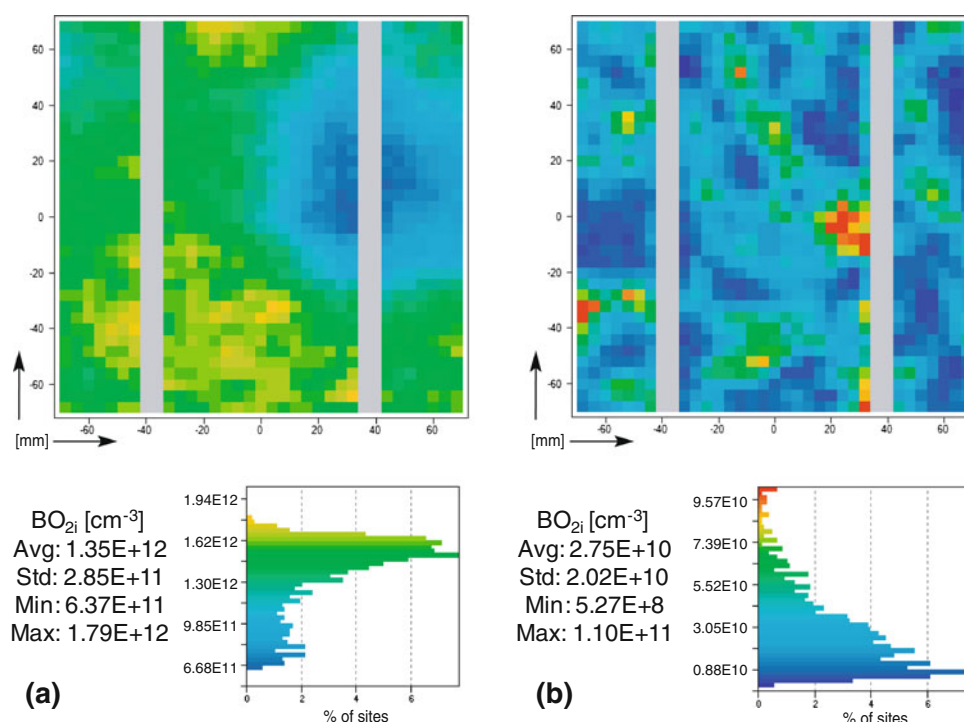


Fig. 4. BO_{2i} concentration maps for two final solar cells with (a) high and (b) low defect concentrations, obtained using ALID and AC SPV diffusion length measurements.

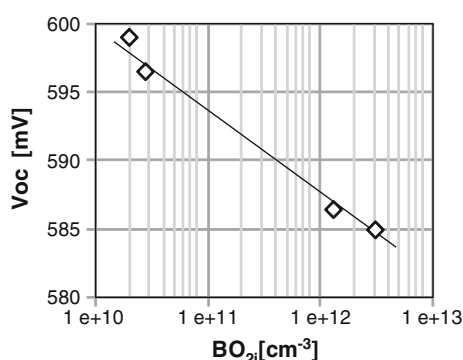


Fig. 5. Open-circuit voltage versus concentration of BO_{2i} defects activated with ALID.

ALID-SPV measurements for two final cells on multicrystalline Si are shown in Fig. 4. The effective BO_{2i} concentration for cell (a) is high, with the average value exceeding 10^{12} defects/cm³. Cell (b) shows a much lower BO_{2i} concentration, with an average value of 2.75×10^{10} defects/cm³.

The ALID cycle can also be used to separate Fe_i and BO_{2i} contributions to open-circuit voltage degradation of solar cells. Cells with high and low BO_{2i} concentrations were treated with ALID. The BO_{2i} concentration was determined from diffusion length values at states 1 and 2 in Table I. In state 2, with the oxygen–boron defect in the highly effective

recombination state and iron inactive, the open-circuit voltage was measured using a short illumination time with 1 sun intensity halogen light to minimize iron activation.

The results in Fig. 5 clearly demonstrate a decrease in V_{oc} with increasing BO_{2i} concentration. This is consistent with a previous study of boron–oxygen light-induced degradation carried out on solar cells fabricated with low-iron-concentration silicon wafers.⁷ With the presently introduced ALID cycle method, it is possible to measure BO_{2i} degradation of solar cells without being restricted to low iron concentrations.

The ALID procedure and specific conditions of defect transformations giving states 1, 2, and 3 in Table I were designed while keeping in mind the high repeatability requirements in manufacturing metrology. Experimental results confirmed very good ALID repeatability. Representative data for a final multicrystalline Si cell are shown in Fig. 6. The BO_{2i} and Fe concentrations for the three repeats are the average values from 141-site wafer maps obtained from AC SPV diffusion length mapping at the appropriate states of ALID, i.e., states 1 and 2 for BO_{2i} and states 2 and 3 for Fe. Maps of these defects are shown in Fig. 7.

To assess the repeatability of wafer-scale mapping it is important to consider not only the map averages of measured parameters but more importantly the repeatability at each site. This is done by plotting the standard deviation of the repeats at

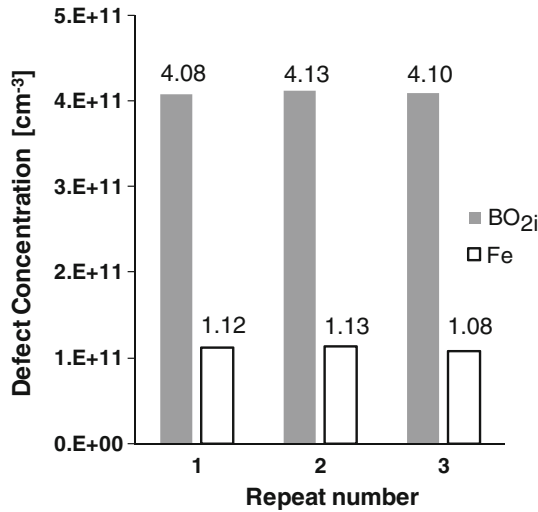


Fig. 6. Average concentration of BO_{2i} and Fe_i defects in three repeats of ALID cycling through defect states 1 to 3 and AC SPV diffusion length mapping measurements of final multicrystalline Si solar cells shown in Fig. 7.

individual sites against the average values of the measured parameters. Such data are shown in Fig. 8 for diffusion lengths at state 1, when both defects are not active, and for state 2, when BO_{2i} is active but Fe remains inactive. The state 3 diffusion length data are not included for clarity, since they overlap the diffusion lengths in state 2. This is a consequence of a relatively low Fe concentration of about 10^{11} atoms/cm³. For this concentration and a diffusion length of about 100 μ m, the iron activation diffusion length shift ΔL is about 5 μ m.

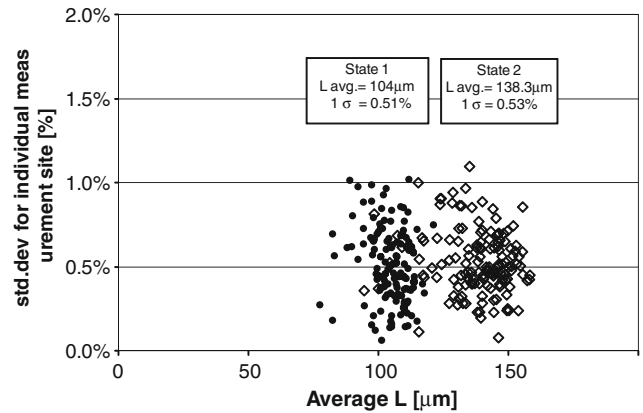


Fig. 8. Individual site repeatability for diffusion length maps in defect states 1 and 2 from three repeats of the ALID cycle.

In Fig. 9 the individual site repeatability is shown. The average standard deviation for all sites of three repeats is 1.8%, and the range of the standard deviation is within 4%. This confirms that the BO_{2i} measurement has sufficient repeatability for mapping of boron–oxygen defects in PV wafers.

One may notice that the standard deviation and the range of the BO_{2i} concentration in Fig. 9 is about four times larger than for the corresponding diffusion length values in Fig. 8. This result is statistically correct. The concentration of BO_{2i} is calculated using Eq. 2, which contains an L^{-2} term that doubles the error. In differential measurements, the L error counts twice. These two factors give an error four times larger for [BO_{2i}] than for L , consistent

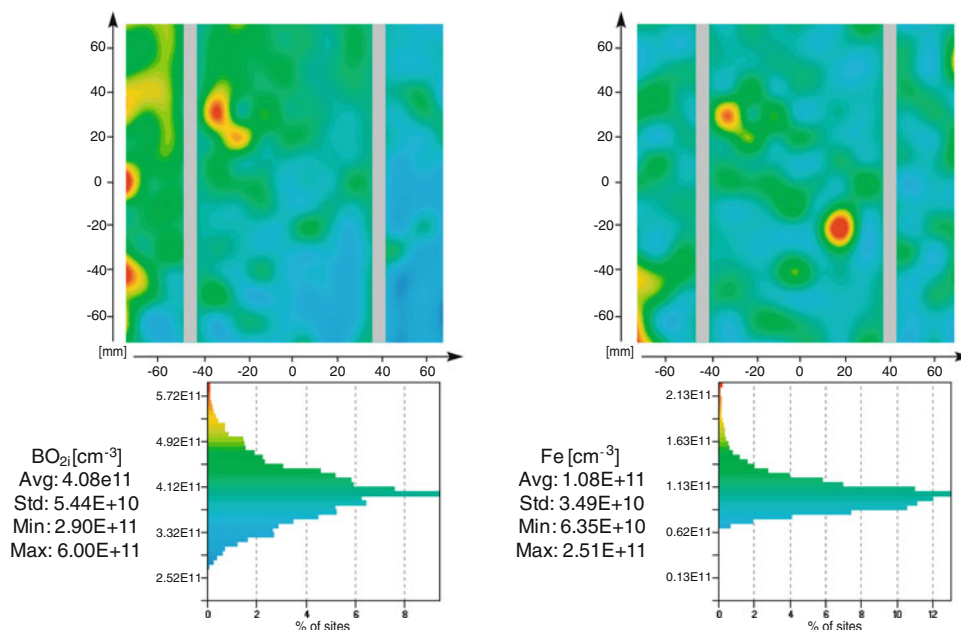


Fig. 7. BO_{2i} and Fe concentration maps of final multicrystalline Si solar cells.

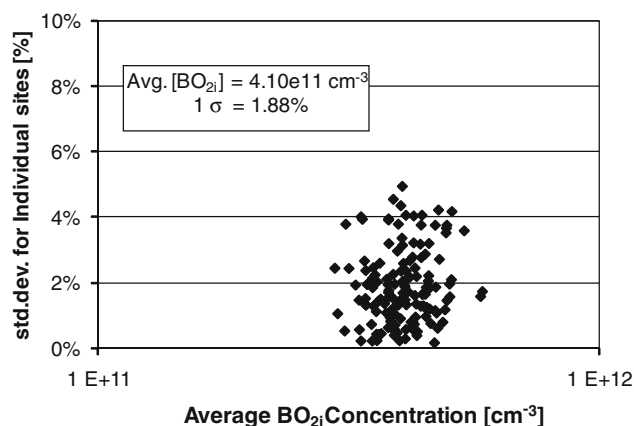


Fig. 9. Individual site repeatability of BO_{21} defect concentration, corresponding to the data in Fig. 8.

with experimental data. We estimate that the repeatability of defect transformation in the ALID process for each defect state is 1% or better.

CONCLUSIONS

We have demonstrated that, by using a carrier photoinjection-induced defect reaction in photovoltaic silicon, the light-induced degradation process can be realized in a highly reproducible way. A corresponding fully reversible accelerated light-induced degradation cycle, ALID, was designed and it was combined with the low-injection-level AC SPV

technique to measure boron–oxygen and boron–iron defects quantitatively. The ALID-SPV method is applicable to as-cut PV wafers and finished solar cells, enabling fast light-induced degradation testing with the unique ability to separate contributions from iron–boron and boron–oxygen defects. The ALID method can also be applied in conjunction with other lifetime measurement techniques, such as microwave photoconductance decay (PCD), light beam induced current (LBIC) or photoluminescence. For these techniques, however, the specific ALID steps may have to be modified to consider different high and low recombination defect activities in measurements with different light injection levels. In this respect, SPV is unique since it operates at well-defined low injection conditions that are insensitive to specific injection level values.

REFERENCES

1. J. Lagowski, P. Edelman, and V. Faifer, *Recombination Lifetime Measurements in Silicon* ed. D.C. Gupta, F.R. Bacher, and W.M. Hughes (West Conshohocken: ASTM STP1340, 1998), p. 125.
2. G. Zoth, *Recombination Lifetime Measurements in Silicon*, ed. D.C. Gupta, F.R. Bacher, and W.M. Hughes (West Conshohocken: ASTM STP1340, 1998), p. 30.
3. L.C. Kimerling and J.L. Benton, *Physica B&C* 116, 297 (1983).
4. J. Schmidt and K. Bothe, *Phys. Rev. B* 69, 24107 (2004).
5. J. Adey, R. Jones, D.W. Palmer, P.R. Briddon, and S. Oberg, *Phys. Rev. Lett.* 93, 055504 (2004).
6. G. Zoth and W. Bergholz, *J. Appl. Phys.* 67, 6764 (1990).
7. K. Bothe and J. Schmidt, *J. Appl. Phys.* 99, 013701 (2006).